Food Chemistry: X 14 (2022) 100318

Contents lists available at ScienceDirect

Food Chemistry: X

journal homepage: www.sciencedirect.com/journal/food-chemistry-x

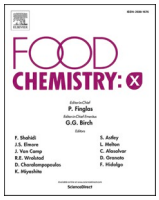

Modification of myofibrillar protein gelation under oxidative stress using combined inulin and glutathione

Wenhui Ma [a,1], Qi Yang [a,1], Xin Fan [a], Xianqi Yao [b], Jiwei Kuang [a], Cong Min [a], Yungang Cao [a,*], Junrong Huang [a,*]

[a] School of Food and Biological Engineering, and Natural Food Macromolecule Research Center, Shaanxi University of Science and Technology, Xi'an 710021, China
[b] Linyi Jinluo Win Ray Food Co., Ltd., Linyi 276036, China

ARTICLE INFO

Keywords:
Myofibrillar protein
Oxidation
Inulin
Glutathione
Gelation

PubMed CID:
Glutathione (PubChem CID: 124886)
Inulin (PubChem CID: 132932783)
PIPES (PubChem CID: 156619641)
DNPH (PubChem CID: 3772977)
Trolox (PubChem CID: 40634)
Dithiothreitol (PubChem CID: 446094)
EGTA (PubChem CID: 6207)

ABSTRACT

The effects of inulin (1.5%), glutathione (GSH, 0.05%), and their combination (1.5% inulin + 0.05% GSH) on the conformational structure and gel performance of pork myofibrillar protein (MP) under oxidation condition were examined. The addition of GSH significantly prevented oxidation-induced carbonylation, reduction of α-helix content, and protein aggregation. As a result, treatment with GSH significantly reduced the particle size of oxidized MP by 35%, increased the solubility by 17.3%, and improved the gelling properties. The presence of inulin also obviously enhanced the gelling behavior of MP under oxidation condition, although it could hardly inhibit the modification of MP structure caused by oxidation. Treatment with inulin + GSH exhibited the highest cooking yield (84.2%) and the best textural characteristics, with a denser and more uniform network structure comprising evenly distributed small pores. The findings of this study provide a useful method for processing meat protein gel products with better oxidative stability and textural properties.

1. Introduction

Emulsion-type sausages are well-received by the market and the consumers mainly due to their palatability, flavor and rich nutrition content. However, traditional emulsion-type sausages contain 15% ~30% animal fat and are particularly high in saturated fatty acids and cholesterol (Cao, Ai, True, & Xiong, 2018; Zhuang et al., 2018). Excessive intake of such types of food has been linked to an increasing incidence of the onset of several kinds of diseases, such as hypertension, obesity and cardiovascular disease (Berasategi, Navarro-Blasco, Calvo, Cavero, Astiasaran, & Ansorena, 2014; Houston et al., 2011). Direct reduction of animal fat content in emulsion-type sausages results in increased cooking loss, poor consumer acceptability and deterioration in flavor. Therefore, a variety of fat substitutes have been used to fix quality issues in low-fat emulsified meat products.

Among these substitutes, dietary cellulose, especially inulin, has aroused great interest of meat researchers and has proven to be efficacious in enhancing the gelling performance of meat proteins and the sensory properties of fat-reduced emulsified sausages (Mendoza, García, Casas, & Selgas, 2001; Tomaschunas, Zörb, Fischer, Köhn, Hinrichs, & Busch-Stockfisch, 2013). Moreover, various studies have confirmed that inulin can inhibit protein denaturation during freeze-drying and frozen storage (Furlán, Padilla, & Campderrós, 2010; Ke, Wang, Ding, & Ding, 2020). However, past research has not yet thoroughly studied the effects of inulin, as a natural antioxidant, on the structure and gelation behavior of meat proteins under oxidative conditions.

In addition to high-fat content not being conducive to human health, the oxidation of fat and protein that occurs during the processing of emulsified sausages poses another challenge, especially protein oxidation, which occurs unnoticed and results in insolubility and reduction in functionality, such as emulsification and gelation (Cao et al., 2021; Xiong & Guo, 2021). Antioxidant strategies utilizing natural antioxidants, e.g., plant polyphenols, polyphosphates, have shown to not always be effective in inhibiting protein oxidation (Cao, Ma, Huang, & Xiong, 2020a; Jiang & Xiong, 2016). Glutathione (GSH), the most abundant non-protein thiol compound, has a strong electron-donating

* Corresponding authors.
E-mail addresses: caoyungang@sust.edu.cn (Y. Cao), huangjunrong@sust.edu.cn (J. Huang).
[1] The authors contributed equally to this work.

https://doi.org/10.1016/j.fochx.2022.100318
Received 13 February 2022; Received in revised form 18 April 2022; Accepted 25 April 2022
Available online 28 April 2022
2590-1575/© 2022 The Author(s). Published by Elsevier Ltd. This is an open access article under the CC BY-NC-ND license (http://creativecommons.org/licenses/by-nc-nd/4.0/).

capacity and, therefore, excellent antioxidant activity (Li, Wei, & Jian, 2004). Additionally, it has been widely reported that GSH can alter the processing properties of dough, mainly by involving itself in the exchange reactions between thiol and disulfide bonds in gluten proteins (Guo, Fang, Zhang, Xu, Xu, & Jin, 2020; Verheyen, Albrecht, Herrmann, Strobl, Jekle, & Becker, 2015). However, in the existing literature, there have been no studies exploring the impact of GSH on the oxidative stability and gelation behavior of meat proteins.

Myofibrillar proteins (MP), the most abundant protein in muscle, predominantly accounts for the textural characteristics of the final muscle foods due to its excellent gelling and emulsifying capacity (Acton, Ziegler, Burge, & Froning, 1983). This study was thus designed to investigate the influence of inulin, GSH and their combination (inulin + GSH) on the oxidative stability, molecular structure and gelation behavior of MP. The study also aimed at examining the textural characteristics and microstructure of the heat-induced MP gel. Gaining insights into these underlying mechanisms can facilitate the development of formulae for restructuring meat products with more healthy and desirable characteristics.

2. Materials and methods

2.1. Materials and reagents

Longissimus dorsi samples (24 h post-mortem) from hybrid barrows of Large White × Duroc × Landrace (6 months) were purchased from Runjia supermarket (Xi'an, China). According to the procedure detailed by Xia, Kong, Liu and Liu (2009), MP was isolated using an extraction buffer (10 mM sodium phosphate, 0.1 M NaCl, 2 mM $MgCl_2$, and 1 mM EGTA, pH 7.0) at 4 °C. Inulin from dahlia tubers (≥ 90% purity, Beijing Solarbio Science & Technology Co., Ltd., Beijing, China), GSH (≥ 99% purity, γ-glutamyl-L-cysteinylglycine, Adamas Reagent Co., Ltd., Shanghai, China), piperazine-N,N′-bis (2-ethanesulfonic acid) (PIPES, ≥ 99% purity, BBI Life Science Corporation, HK, China), including all other reagents used were of analytical grade.

2.2. Sample preparation

MP suspensions (30 mg/mL) with 1.5% inulin, 0.05% GSH and their combination (1.5% inulin + 0.05% GSH) were prepared by adequately mixing different proportions of freshly prepared inulin (15%) and GSH (0.5%) solutions with a stock MP suspension (40 mg/mL) prepared with a PIPES buffer A (15 mM, containing 0.4 M NaCl, pH 6.25). The MP and additives mixture samples were oxidized at 4 °C for 12 h using a Fenton system (10 μM $FeCl_3$, 100 μM ascorbic acid and 10 mM H_2O_2). To terminate the oxidation, 1 mM Trolox was added to the samples (Cao et al., 2020a). The inulin concentration (1.5%) was based on the results of a pre-experiment conducted, where the addition of inulin significantly enhanced the textural characteristics of the heat-induced MP gel under the aforementioned oxidative conditions. The samples that underwent different treatments were named as follows: NonOx (non-oxidized), Ox (oxidized), Ox + Inulin, Ox + GSH and Ox + Inulin + GSH, oxidized in the presence of inulin, GSH and their combination.

2.3. Carbonyl content

The carbonyl content of different treated MP samples was estimated using the 2,4-dinitrophenylhydrazine (DNPH) method (Levine et al., 1990), because carbonyl groups can react with DNPH to form protein hydrazones under acidic conditions. A molar extinction coefficient of 22,000 M^{-1} cm^{-1} was used for carbonyl content calculation.

2.4. Circular dichroism

Far-ultraviolet circular dichroism spectroscopy was carried out using a Chriascan spectrometer (Applied Photophysics Ltd., Surrey, UK) to analyze the secondary structure of the different treated MP samples (Cao et al., 2021). Nitrogen was blown for 30 min before use, and the xenon lamp was turned on. The samples were uniformly diluted to 0.2 mg/mL with a PIPES buffer A and then pipetted into a quartz cell with a 1 cm optical path. After removing the background of the instrument, the samples were scanned from 200 nm to 260 nm. The other parameter settings were as follows: bandwidth (1 nm), step (0.5 nm) and time per point (0.5 s). The solvent was collected twice, and the samples were collected thrice.

2.5. Intrinsic tryptophan fluorescence

The intrinsic tryptophan fluorescence emission spectra (290–400 nm) were determined to reflect different treatment-induced changes in the protein tertiary structure. The protein concentration of the MP suspensions was diluted to 0.4 mg/mL with a PIPES buffer A and then excited at 283 nm using a FluoroMax-4 spectrofluorometer (Horiba Jobin Yvon Inc., Edison, NJ, USA) at 25 °C.

2.6. Sodium dodecyl sulphate–polyacrylamide gel electrophoresis

Sodium dodecyl sulphate–polyacrylamide gel electrophoresis (SDS–PAGE) was performed to reveal the cross-linking and polymerization of the different treated MP samples. First, the different treated MP suspensions (2 mg/mL) were mixed thoroughly with the sample buffer at a ratio of 1:1. Second, the mixed liquids were boiled for 3 min and cooled at room temperature. Third, following centrifugation at 1000×*g* for 2 min, the supernatant (25 μL) of the mixed liquids was injected into each groove in a 4% concentrated gel and separated with the help of 12% resolving gel.

2.7. Particle size analysis

The particle size distribution of the different treated MP samples was determined through a Mastersizer 2000 laser particle size analyzer (Malvern Instruments Co., Ltd., Worcestershire, U.K.) based on static light scattering at room temperature. The MP samples were adjusted to 2 mg/mL with a PIPES buffer A and dispersed in double-distilled water to avoid multiple scattering. The refractive indices of the MP particles and the dispersant were set to 1.434 and 1.330, respectively.

2.8. Protein solubility determination

The different treatment-induced protein solubility changes were revealed using the classical centrifugation method detailed by Gao, Huang, Zeng and Brennan (2019). Diluted MP suspensions (2 mg/mL) were centrifuged (5000 g) at 4 °C for 15 min. The protein concentration of the supernatant after centrifugation was measured using Biuret method. Protein solubility (%) was calculated using the following formula:

$$\text{Protein solubility } (\%) = \frac{\text{protein concentration of the supernatant}}{\text{protein concentration of the original MP suspension}} \times 100\%$$

2.9. Dynamic rheological behavior test

The dynamic rheological parameters of the MP samples (30 mg/mL) were analyzed using a Haake Mars 60 rheometer (Thermo Scientific, Germany), equipped with a 35 mm upper parallel plate. After removing the air bubbles by centrifuging (at 1000 g and 4 °C for 2 min), 1.5 mL of the MP samples was carefully placed between the two parallel plates. The gap was set to 1 mm, and silicone oil was used to seal the edges of the gap to avoid dehydration. Under the oscillatory mode of CD-AutoStrain, the MP samples were heated from 20 °C to 75 °C at a

heating rate of 1 °C/min. The other test parameters were a fixed frequency of 0.1 Hz and a controlled strain of 2%. The storage modulus (G′) and the phase angle (tanδ) were recorded.

2.10. Texture profile analysis

Following centrifugation at 1000*g* at 4 °C for 2 min for removing the air bubbles, about 5 g of 30 mg/mL MP sols was transferred into small glass bottles, gently sealed with a cork, heated in a water bath from 20 °C to 75 °C at a heating rate of ~1 °C/min. The formed gels were then taken out and immediately cooled in an ice-water bath followed by incubation in a refrigerator at 4 °C for 12 h. The indicators were finally measured.

Texture of the MP composite gels—A very thin shovel was used to gently segregate the gel from the walls of the small glass bottles. The gel was thus removed and placed on a flat plate for texture determination. The texture profile analysis of the heat-induced gels was carried out using a texture analyzer (TA.XT plus, Stable Micro Systems Ltd., Surrey, UK), equipped with a P/75 aluminum alloy probe. The MP gels were compressed to 30% of their initial height by introducing a trigger force of 10 g. The pre-test, test and post-test speeds measured were 2.0 mm/s. Hardness was defined as the maximum peak force during the first compression cycle. Springiness was defined as the ratio of the second compression distance to the first compression. Cohesiveness was calculated as the ratio of the positive force area during the second compression to that during the first compression. Resilience was defined as ratio of upstroke-to-downstroke energy of the first compression. Chewiness was defined as hardness × cohesiveness × springiness.

2.11. Cooking yield and whiteness measurement

Cooking yield (%) was tested and expressed as the weight percentage of the heat-induced gel (gm) over the original MP sol (gm).

Hunter L*(lightness), a*(redness/greenness), and b*(yellowness/blueness) color of the gels was determined on the surface of the MP gels at an arbitrary place using a CM-5 colorimeter (Konica Minolta Sensing, Inc., Tokyo, Japan), and the whiteness was calculated using the following equation:

$$Whiteness = 100 - \sqrt{(100 - L^*)^2 + a^{*2} + b^{*2}}$$

2.12. Raman spectrometric measurements

Raman spectra (600 cm^{-1}–2000 cm^{-1}) were recorded using a laser microscopic Raman imaging spectrometer (DXR2, Thermo Fisher Scientific, USA). The detailed parameter settings have been highlighted in the literature by Cao et al. (2020a) as follows: laser source DXR 785 nm; microscope 10×/0.25 BD; laser power 30 mW; aperture 50 μm slit; collect exposure time 30 s and sample exposures 3 times. According to Xia et al. (2019), the collected Raman spectra data was analyzed, and the percentages of the secondary structures were calculated.

2.13. Environmental scanning electron microscope

The micromorphology characteristics of the set heat-induced MP gels were observed according to the procedure described by Zhuang et al. (2018). The MP gels were trimmed to small cubes, fixed with a 2.5% glutaraldehyde solution for 4 h, washed four times using 0.1 M phosphate buffer (pH 7.4) for 10 min, dehydrated in a series of ethanol for 30 min, freeze-dried and sprayed with a thin layer of gold. The three regions of each gel sample were imaged using an environmental scanning electron microscope (ESEM) (Q45, FEI Inc., Hillsboro, Orlando, USA).

2.13. Statistical analysis

All experiments were conducted at least thrice, except in specific circumstances, where more measurements were taken. The experimental data was processed using the general linear model procedure (Statistix 9.0 was the software employed, Analytical Software, Tallahassee, Florida, USA). A significant difference between the means was determined using the least significant difference, all-pairwise multiple comparisons, at 5% significance level ($P < 0.05$). The data was plotted using the SigmaPlot 14.0 software.

3. Results and discussion

3.1. Carbonyls

The change in carbonyl content is a widely used biochemical indicator to measure the extent of protein oxidation. As shown in Fig. 1a, the carbonyl content of the non-oxidized MP was 2.10 nmol/mg protein, and it increased to 4.21 nmol/mg when exposed to •OH. This is because many amino acid side chain groups in MP (e.g., NH_2 and NH) are converted to carbonyls when subjected to free radicals (Cao et al., 2020a; Estevez, 2011). The presence of inulin did not prevent an increase in carbonyl content induced by oxidation. However, the incorporation of GSH and inulin + GSH ($P < 0.05$) suppressed the •OH-induced carbonyl formation by 25.7% and 25.4%, respectively, because GSH can efficiently scavenge the free radicals (Jiao & Wang, 2000). This prevented the MP from being attacked by •OH and suppressed the conversion of amino acid residues in protein side chain groups into carbonyl groups.

3.2. Secondary structure

From Fig. 1b, it can be seen that the circular dichroism (CD) spectra of all MP samples exhibited negative peaks at about 222 nm, indicating the existence of abundant α-helix structures in the MP samples (King & Lehrer, 1989). Compared to non-oxidized control, oxidation significantly reduced the absolute peak values of 222 nm (Fig. 1b) and drastically lowered the α-helix content by 13.0% (Fig. 1c), accompanied by an obviously increase in β-sheets and random coil structures ($P < 0.05$). Sun, Zhou, Sun and Zhao (2013) also reported that protein oxidation promotes the unfolding of α-helix to form β-sheets and random coil structures. The presence of inulin, GSH and inulin + GSH significantly improved α-helix content by 12.4%, 14.6% and 17.4%, respectively, compared to oxidized control. These results suggest that the presence of inulin and GSH has the potential to inhibit oxidation-induced unwinding of α-helix structures in proteins. Combining inulin + GSH revealed the maximum protection.

3.3. Intrinsic tryptophan fluorescence

Intrinsic tryptophan fluorescence was applied to analyze the impact of different treatment methods on the conformational changes of MP. As illustrated in Fig. 1d, the intrinsic tryptophan fluorescence intensity of MP decreased obviously ($P < 0.05$) after being attacked by •OH, indicating that oxidation-induced protein unfolding resulted in the exposure of tryptophan residues to a polar environment (Cao et al., 2020b; Sun et al., 2013). The presence of inulin, GSH and inulin + GSH had no protective effect on the oxidation-induced conformational changes; instead, the addition of inulin with or without GSH tended to promote the attenuation of fluorescence intensity due to oxidation. This could be because inulin contains multiple hydroxyl groups that can increase the polarity of the surrounding environment or binding to the active functional groups in tryptophan residues, causing fluorescence quenching (Zhang, Dong et al., 2020).

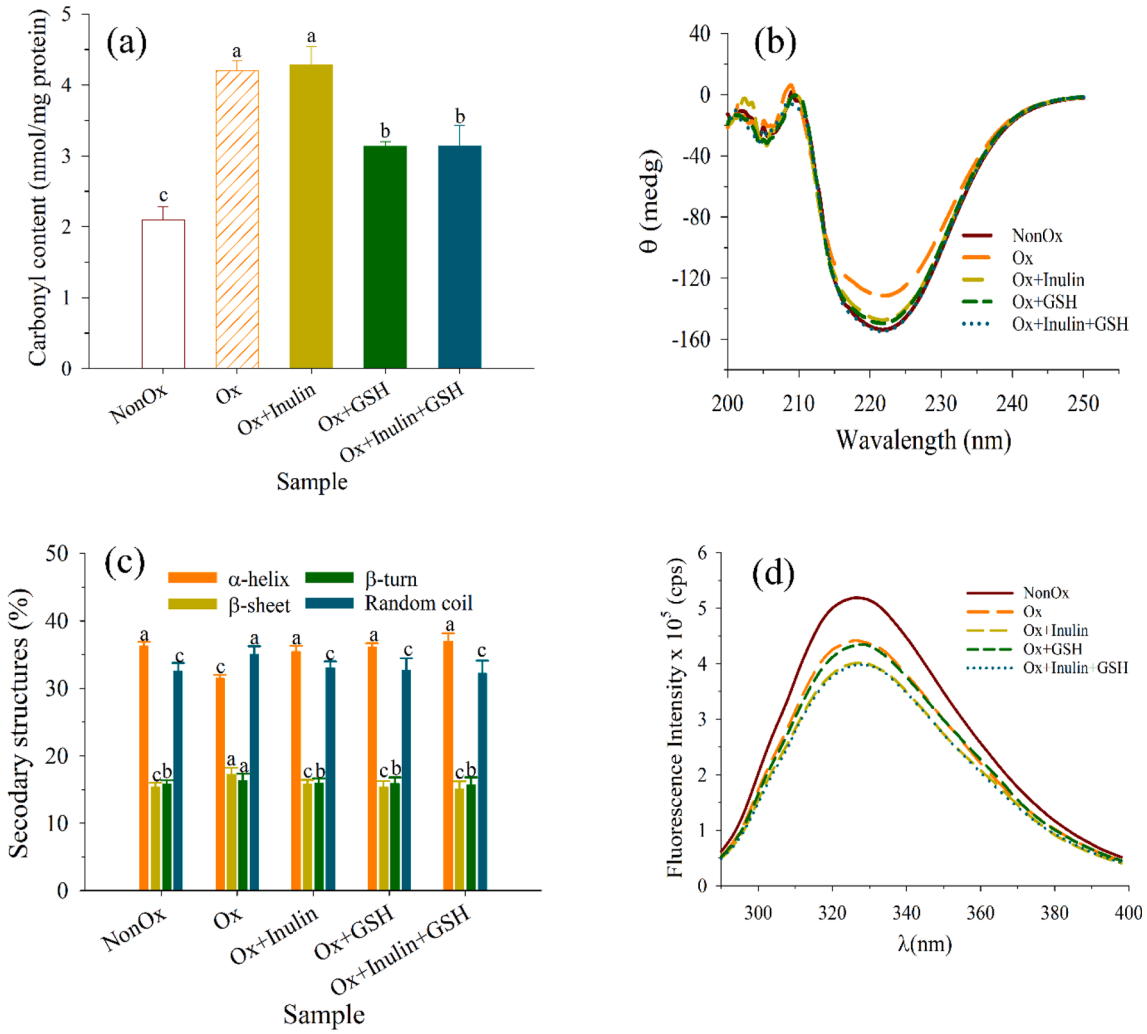

Fig. 1. Carbonyl content (a), circular dichroism (CD) spectra (b), percentages of secondary structures (c) and intrinsic tryptophan fluorescence (d) of MP, as influenced by oxidation, with the incorporation of inulin, GSH and their combination (inulin + GSH). Different lowercase letters (a–c) indicate significant differences ($P < 0.05$).

3.4. Protein cross-linking

The protein patterns of the different treated MP samples in the absence and presence of dithiothreitol (DTT) are shown in Fig. 2a. In the absence of DTT (-DTT), compared to the non-oxidized samples, oxidation significantly accelerated protein cross-linking as evident from the loss of both myosin heavy chain (MHC) and actin bands. In the presence of DTT (+DTT), most of the lost MHC and actin were recovered, but a small number of high polymers were still noticed at the top of the concentrated gel, indicating that oxidation induced the cross-linking of proteins, mainly through disulfide bonds (S—S) and little through other covalent bonds—for instance, carbonyl–NH_2 and Tyr–Tyr (Cao et al., 2020a; Estevez, 2011).

The presence of inulin could not restrain •OH-induced protein cross-linking and aggregation. However, the presence of GSH, with or without inulin, improved the band intensity of MHC and actin (-DTT) and significantly reduced the remnant high polymers under the reducing conditions (+DTT). These results once again prove that GSH can effectively prevent •OH-induced protein oxidation, including the conversion of SH to S—S and the formation of other covalent bonds.

3.5. Particle size

The protein particle size distribution can be used to characterize the degree of aggregation or degradation of proteins. As shown in Fig. 2b, the peak of the particle size distribution shifted to the right (larger particle sizes) after the MP was exposed to the Fenton system, suggesting that oxidation causes protein aggregation. Some previous studies, where different oxidation systems were used, have also reported a similar pattern of oxidation-induced increase in the particle size of MP (Bao, Boeren, & Ertbjerg, 2017; Li, Wu, & Wu, 2020). The presence of additives (inulin, GSH and inulin + GSH) significantly suppressed the increase in particle size induced by oxidation while the presence of GSH exhibited the best inhibition effect. It should be noted that the particle size distribution curve of Ox + Inulin was very similar to that of Ox + Inulin + GSH. This could be due to the greater impact of inulin on the conformation of MP, as supported by the results of intrinsic tryptophan fluorescence (Fig. 1d).

3.6. Protein solubility

As shown in Fig. 2c, the solubility of non-oxidized MP was 54.4% after being attacked by •OH, a significant reduction in solubility of 22.4% was observed ($P < 0.05$). The addition of inulin did not inhibit •OH-induced solubility reduction; however, the presence of GSH, with or without inulin, improved the solubility of the oxidized MP up to 48.5% and 49.5%, respectively. As mentioned above, the introduction of inulin had no protective effect on oxidation-induced carbonyl formation

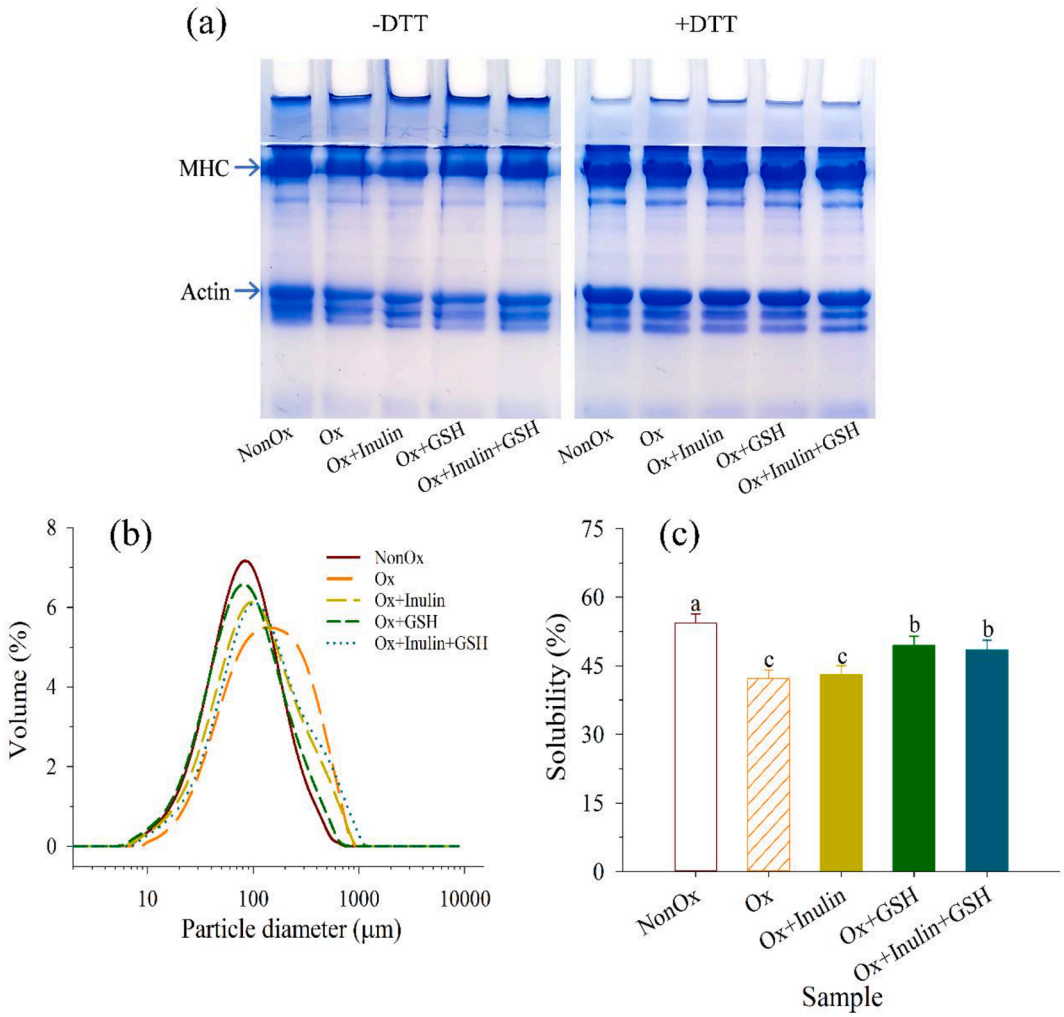

Fig. 2. SDS–PAGE patterns (a), particle size distribution (b) and solubility (c) of MP, as influenced by oxidation, with the incorporation of inulin, GSH and their combination (inulin + GSH). Different lowercase letters (a − c) indicate significant differences ($P < 0.05$).

(Fig. 1a) and protein cross-linking and aggregation (Fig. 2a). GSH treatment, however, significantly suppressed •OH-induced carbonyl formation and protein aggregation (Fig. 2a, 2b). These findings indicate the effects of different additive treatment options on protein solubility.

3.7. Dynamic rheological properties

The rheological properties of the MP suspensions can reflect the influence of different treatments on gel formation and gel elasticity. The dynamic rheological patterns of the MP suspensions that underwent different treatments during the process of heating are presented in

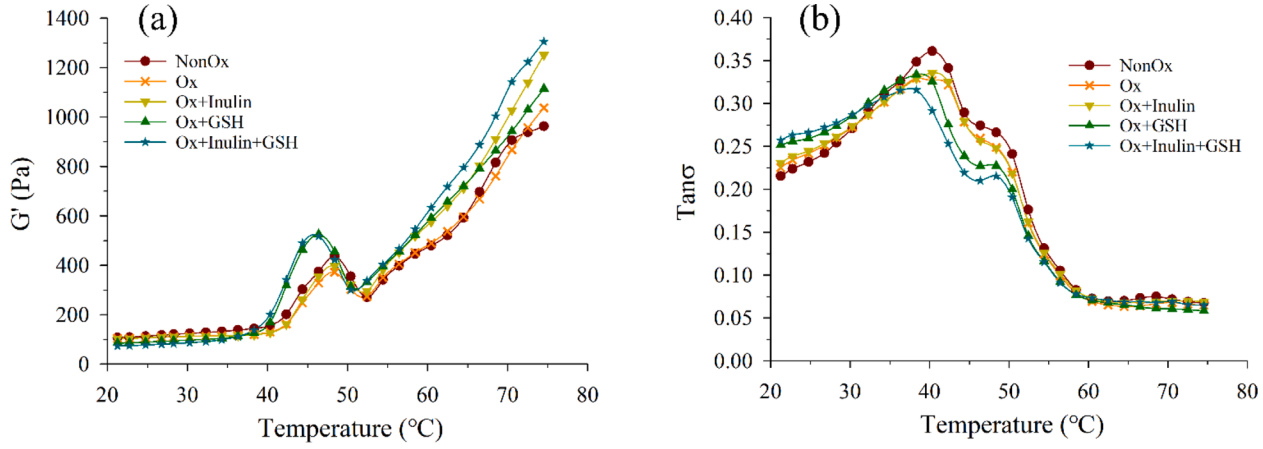

Fig. 3. Storage modulus (G′, a) and tangent delta (tanδ, b) of MP sols during thermal gelation, as influenced by oxidation, with the incorporation of inulin, GSH and their combination (inulin + GSH).

Fig. 3. The non-oxidized MP sample exhibited a typical G′ curve passing through three different stages. In the first stage, the G′ value gradually rose and achieved a transition peak at a temperature range of 40 °C–53 °C due to the denaturation and aggregation of the myosin heads (S1) to form a weak gel network (Egelandsdal, Fretheim, & Samejima, 1986; Zhang, Dong et al., 2020). In the subsequent stage, the G′ value sharply dropped to a trough at about 53 °C due to the denaturation of light meromyosin, which resulted in the temporary collapse of the previously formed weak gel network (Liu, Zhao, Xie, & Xiong, 2011). In the last stage, the G′ value gradually increased over the 53 °C–75 °C temperature range, which can be attributed to the formation of a permanent, irreversible and stronger gel network (Egelandsdal et al., 1986; Tolano-Villaverde, Ezquerra Brauer, Ocaño-Higuera, & Torres, 2016).

After being attacked by •OH, the peak value of the G′ curve slightly decreased, whereas the final G′ value slightly increased, indicating that the head-head interactions were repressed while the tail–tail interactions were enhanced (Xu et al., 2020). Treatment with additives had no visible effect on the type of G′ curve; however, such treatment changed the peak, the final G′ values and significantly improved the elasticity of the oxidized MP (Fig. 3a). The incorporation of inulin had almost no influence on the peak G′ value; however, it promoted a rise in the value of G′ in the last stage, suggesting that the addition of inulin favored the tail–tail interaction during heating. Zhang, Dong et al. (2020) also found that the addition of inulin obviously improved the final G′ values of the porcine myosin systems. They proposed that inulin absorbed part of the water and increased the relative concentration of myosin in the system, which could benefit cross-linking among proteins and aid the formation of the gel network (Villamonte, Simonin, Duranton, Chéret, & De Lamballerie, 2013). It was interesting to observe that the addition of GSH, with or without inulin, made the transition peak of the oxidized MP shift from 49 °C to 46 °C and significantly elevated the peak and the final G′ values, indicating that both head-head and tail–tail interactions were enhanced. This could be related to the antioxidant activity of GSH and the important role played by GSH during the interchange of sulfhydryl and disulfide bonds in the oxidized MP (Guo, Fang, Zhang, Xu, Xu, & Jin, 2020). Treatment with inulin and GSH exhibited the highest final G′ value, implying their synergistic effect in improving the gelling properties of the oxidized MP.

The tanδ value represents the ratio of G″/G′ in the thermal gelation processing of MP suspensions. A higher tanδ value indicates that the sample is more viscous or less elastic (Cao et al., 2020b; Zhang, Dong et al., 2020). As shown in Fig. 3b, the tan δ value of the non-oxidized MP suspension gradually increased and reached a transition peak at 39 °C. It soon decreased significantly with an increase in temperature until 75 °C. After being attacked by •OH, the initial tanδ value of the MP suspension was slightly higher; this is because oxidation induced the structural unfolding of the MP (Fig. 1b, c) and resulted in a bulkier hydrodynamic volume (Cao et al., 2020a). The incorporation of inulin alone had almost no influence on the tanδ value throughout the heating process. The presence of GSH, with or without inulin, significantly improved the initial tanδ value, suggesting that GSH enhances the viscosity of the oxidized MP suspension system at room temperature. All of the viscous treatments had almost no influence on the type of tanδ curve, and the final tanδ values of all MP samples were close to each other, which confirmed that heat treatment transformed all the MP sols into elasticity-dominant gels.

3.8. Textural properties

The textural properties of MP gels, as influenced by the hydroxyl radical, with the incorporation of inulin, GSH and their combination (inulin + GSH) are shown in Table 1. Compared to non-oxidized control, the hardness, springiness, cohesiveness, chewiness and resilience of the oxidized MP gel was significantly reduced ($P < 0.05$) by 13%, 21.3%, 27.7%, 27.7% and 32.3%, respectively. These results are inconsistent with the rheology results, because the G′ is a measure of shear stress only (Cao et al., 2020a). The incorporation of inulin, GSH and inulin + GSH significantly increased ($P < 0.05$) all the textural characteristics of the oxidized MP gel. Among these, GSH and inulin + GSH treatments exhibited further enhancement in protective effect, and their hardness and chewiness were even superior to those of the non-oxidized MP gel. Similar results have been reported by Zhang, Dong et al. (2020), who found that inulin addition (0%–5%) significantly enhanced the gel strength of porcine myosin; by Wang et al. (2021), who found that water-insoluble dietary fibers (90 μm, 1.5% and 3%) significantly improved the gel strength of duck myofibrillar proteins; and by He, Liu, Zhao, Li and Wang (2021), who revealed that the incorporation of pectin (0.1 and 0.5%) obviously strengthened the textural properties of ginkgo seed protein.

Table 1
Textural properties of MP gels, as influenced by oxidation, with the incorporation of inulin, glutathione (GSH), and their combination (inulin + GSH).

Sample*	Hardness (g)	Springiness	Cohesiveness	Chewiness	Resilience
NonOx	83.5 ± 2.00^{a}	0.195 ± 0.020^{a}	0.287 ± 0.01^{a}	3.14 ± 0.11^{bc}	0.122 ± 0.018^{a}
Ox	70.4 ± 4.02^{b}	0.149 ± 0.007^{b}	0.201 ± 0.01^{d}	2.61 ± 0.03^{c}	0.080 ± 0.002^{c}
Ox + Inulin	84.3 ± 4.14^{a}	0.175 ± 0.007^{a}	0.227 ± 0.01^{c}	3.80 ± 0.35^{b}	0.096 ± 0.004^{bc}
Ox + GSH	86.4 ± 2.75^{a}	0.190 ± 0.012^{a}	0.259 ± 0.01^{b}	5.38 ± 0.14^{a}	0.112 ± 0.005^{ab}
Ox + Inulin + GSH	88.8 ± 3.16^{a}	0.181 ± 0.016^{a}	0.248 ± 0.02^{bc}	5.26 ± 0.79^{a}	0.112 ± 0.012^{ab}

*NonOx (non-oxidized), Ox (oxidized), Ox + Inulin, Ox + GSH and Ox + Inulin + GSH, oxidized with the incorporation of inulin, GSH and inulin + GSH. Different lowercase letters (a–d) in the same column indicate significant differences ($P < 0.05$).

3.9. Cooking yield and color

As shown in Fig. 4, a 21.5% reduction ($P < 0.05$) in the cooking yield of the MP gel was observed after being attacked by •OH. Compared to oxidized control, the addition of additives (inulin, GSH and inulin + GSH) improved the cooking yield of the MP gel by 10.8%, 15.1% and 15.8%, respectively. Zhang, Dong et al. (2020) reported findings consistent with the above results: Inulin can significantly enhance the water holding capacity of porcine myosin gel in a dose-dependent

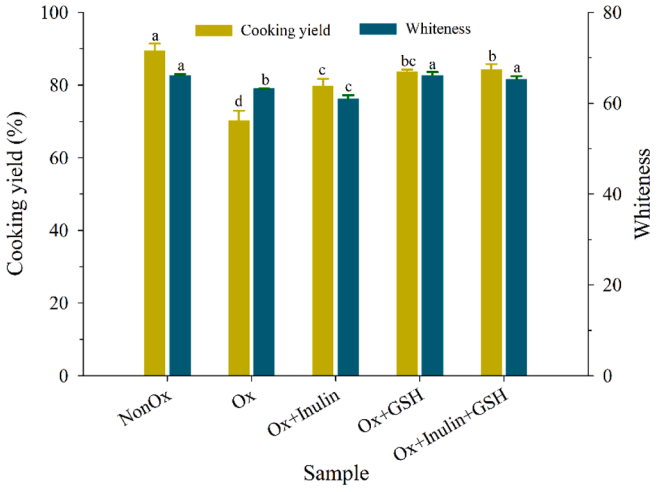

Fig. 4. Cooking yield and color of MP gels, as influenced by oxidation, with the incorporation of inulin, GSH and their combination (inulin + GSH). Different lowercase letters (a–d) indicate significant differences ($P < 0.05$).

manner. The anti-oxidation property of GSH to prevent oxidation-induced deterioration in gel-forming ability and the ability of inulin to physically entrap water were considered to be the primary causes for the enhancement of water holding capacity (Meyer, Bayarri, Tárrega, & Costell, 2011; Zhang, Dong et al., 2020).

After being attacked by •OH, the whiteness of the MP gel decreased by 4.4% ($P < 0.05$) over the non-oxidized MP gel, which can be linked to the oxidation of protein and residual phospholipids in the MP (Cao et al., 2020a; Hwang, Lai, & Hsu, 2007). Treatment with inulin did not prevent •OH-induced color deterioration and further reduced the gel whiteness. The color of the oxidized products of inulin could be a reason. The incorporation of GSH significantly eliminated the reduction of gel whiteness induced by oxidation due to its excellent oxidation resistance—for instance, inhibition of carbonyl formation (Fig. 1a). When combined with GSH, the addition of inulin had an adverse impact on gel whiteness, which was almost completely eliminated. This phenomenon could be attributed to the presence of GSH, which inhibited the oxidation of protein and inulin.

3.10. Secondary structure in MP gels

In recent years, Raman spectroscopy has been widely applied to provide structural information of protein in sols or in gels, where the secondary structure of proteins is of particular concern. Many studies have suggested that the textural characteristics and the water holding capacity of gels are associated with the secondary structure of proteins in gels (Chen & Han, 2011; Zhang, Ma, & Sun, 2020). The Raman spectrum (600 cm^{-1}–1800 cm^{-1}) of the different treated MP gels is illustrated in Fig. 5a. The Raman spectral band 1600 cm^{-1}–1700 cm^{-1} is designated as the amide I band. The spectral bands 1645 cm^{-1}–1660 cm^{-1}, 1665 cm^{-1}–1680 cm^{-1}, 1660 cm^{-1}–1665 cm^{-1} and 1680 cm^{-1}–1690 cm^{-1} are assigned to the α-helix, β-sheet, β-turn and random coil, respectively (Herrero, 2008; Zhang, Ma, & Sun, 2020).

The quantitative results of protein secondary structures of the different treated MP gels are presented in Fig. 5b. Upon oxidative treatment, the α-helix and β-sheet contents of the MP gel decreased from 36.34% and 37.11% to 34.93% and 31.99%, respectively; while the β-turn and random coil structures' content increased from 7.98% and 18.57% to 11.64% and 21.44%, respectively ($P < 0.05$). Similar results were obtained in previous studies (Cao et al., 2020a; Xia et al., 2019). It is believed that the deterioration in textural properties of the oxidized MP gel was closely linked to the reduction in β-sheet content caused by oxidation treatment before heating (Kobayashi, Mayer, & Park, 2017). The presence of antioxidants (inulin, GSH and inulin + GSH) significantly prevented the reduction of α-helix and β-sheet and increased the β-turn and random coil of the oxidized MP gel. A higher proportion of

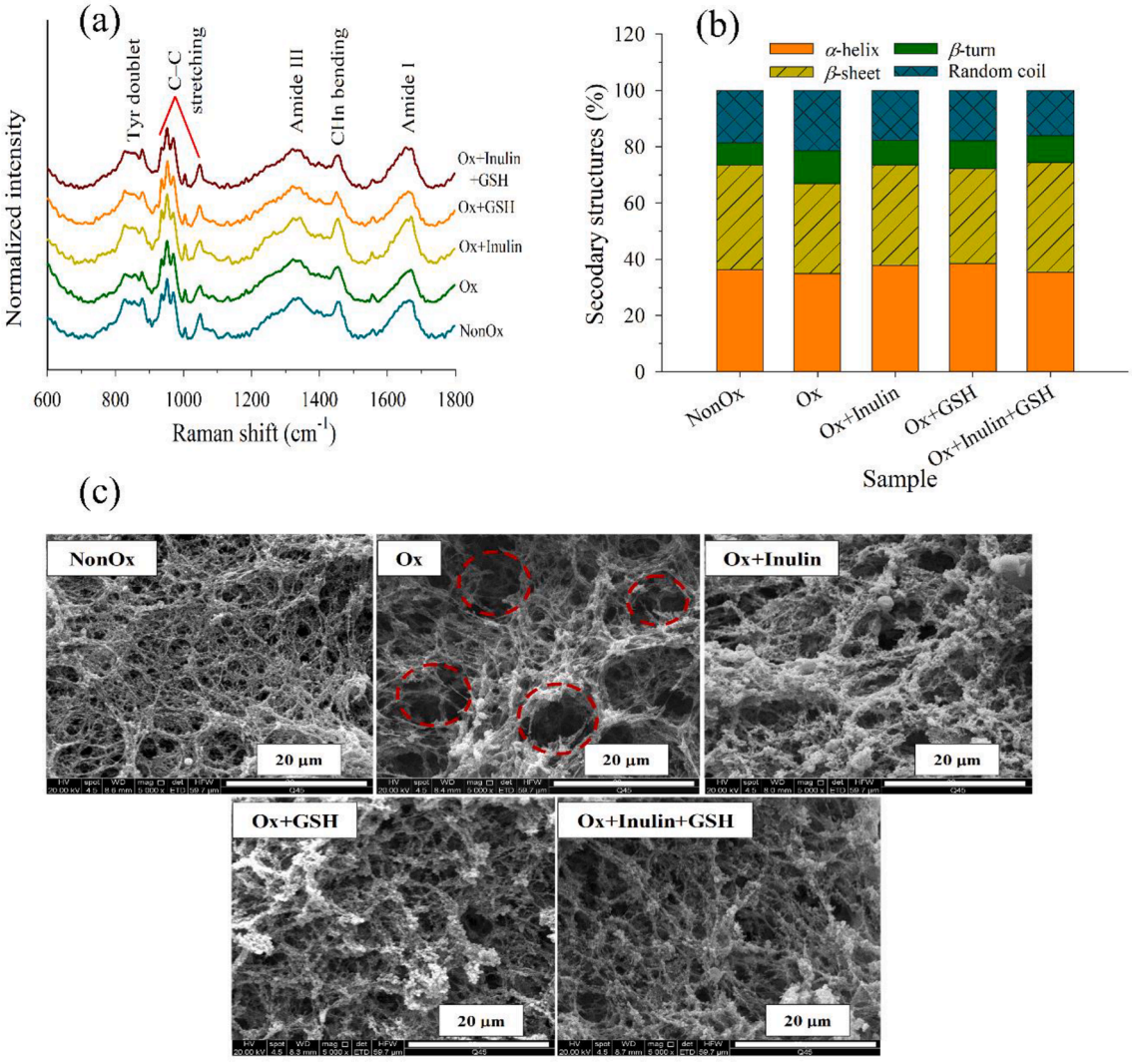

Fig. 5. Raman spectrum (600 cm^{-1}–1800 cm^{-1}, a), percentages of secondary structures (b) and ESEM images (c) of MP gels, as influenced by oxidation, with the incorporation of inulin, GSH and their combination (inulin + GSH).

β-sheets probably indicates enhanced hydrophobic interactions taking place among proteins (Herrero, 2008) and is closely associated with an improvement in textural characteristics (Table 1) and cooking yield (Fig. 4) of the oxidized MP gel.

3.11. Gel microstructure

As shown in Fig. 5c, the non-oxidized MP gel exhibited a compact and ordered structure with evenly distributed micropores. However, the network structure of the oxidized MP gel was very irregular and heterogeneous, among which the inhomogeneous macropores were visible, which explains the significantly reduced cooking yield (Fig. 4) and textural properties (Table 1). Compared to oxidized control, the oxidized MP gels combined with inulin, GSH and inulin + GSH exhibited a more uniform and compact microstructure with smaller water pores, followed by inulin + GSH, GSH and inulin in the descending order. In a similar vein, Zhang, Dong et al. (2020) found that heat-induced gel from porcine myosin, introduced with 2% inulin, displayed a finer and smoother microstructure with uniformly distributed smaller pores. The presence of GSH, with or without inulin in MP sols, restrained •OH-induced changes, including carbonyl formation, conformational unfolding and polymerization. All these changes contributed to the formation of better gel microstructures.

4. Conclusions

Treatment with GSH significantly prevented oxidation-induced carbonylation and protein insolubility, whereas treatment with inulin alone showed no protective effect. The incorporation of different additives (inulin, GSH and inulin + GSH) effectively eliminated oxidation-induced changes in the secondary structures and mean particle sizes of the MP. As a result, all additive treatments improved the rheological properties of the oxidized MP. Inulin + GSH treatment was found to be the most effective in terms of enhancing the textural properties and cooking yield of the corresponding heat-induced gels. It is important to note that the addition of inulin reduced the gel whiteness probably due to the color of its oxidation products; however, the addition of GSH completely inhibited oxidation-induced reduction in gel whiteness and eliminated the negative effects on gel whiteness caused by the introduction of inulin. Therefore, a combination of inulin and GSH is recommended when processing meat products to avoid oxidation-induced changes that lead to the quality deterioration of meat proteins.

Declaration of Competing Interest

The authors declare that they have no known competing financial interests or personal relationships that could have appeared to influence the work reported in this paper.

Acknowledgments

The authors would like to thank the National Natural Science Foundation of China (grant number 31801480) for funding this study.

References

Acton, J. C., Ziegler, G. R., Burge, D. L., & Froning, G. W. (1983). Functionality of muscle constituents in the processing of comminuted meat products. *Critical Reviews in Food Science and Nutrition, 18*(2), 99–121. https://doi.org/10.1021/c160024a013

Bao, Y., Boeren, S., & Ertbjerg, P. (2017). Myofibrillar protein oxidation affects filament charges, aggregation and water-holding. *Meat Science, 135*, 102–108. https://doi.org/10.1016/j.meatsci.2017.09.011

Berasategi, I., Navarro-Blasco, I., Calvo, M. I., Cavero, R. Y., Astiasaran, I., & Ansorena, D. (2014). Healthy reduced-fat Bologna sausages enriched in ALA and DHA and stabilized with Melissa officinalis extract. *Meat Science, 96*(3), 1185–1190. https://doi.org/10.1016/j.meatsci.2013.10.023

Cao, Y., Ai, N., True, A. D., & Xiong, Y. L. (2018). Effects of (−)-epigallocatechin-3-gallate incorporation on the physicochemical and oxidative stability of myofibrillar protein-soybean oil emulsions. *Food Chemistry, 245*, 439–445. https://doi.org/10.1016/j.foodchem.2017.10.111

Cao, Y., Li, B., Fan, X., Wang, J., Zhu, Z., Huang, J., & Xiong, Y. L. (2021). Synergistic recovery and enhancement of gelling properties of oxidatively damaged myofibrillar protein by L-lysine and transglutaminase. *Food Chemistry, 20*, Article 129860. https://doi.org/10.1016/j.foodchem.2021.129860

Cao, Y., Ma, W., Huang, J., & Xiong, Y. L. (2020a). Effects of sodium pyrophosphate coupled with catechin on the oxidative stability and gelling properties of myofibrillar protein. *Food Hydrocolloids, 104*, Article 105722. https://doi.org/10.1016/j.foodhyd.2020.105722

Cao, Y., Ma, W., Wang, J., Zhang, S., Wang, Z., Zhao, J., … Zhang, D. (2020b). Influence of sodium pyrophosphate on the physicochemical and gelling properties of myofibrillar proteins under hydroxyl radical-induced oxidative stress. *Food & Function, 11*(3), 1996–2004. https://doi.org/10.1039/C9FO02412C

Chen, H., & Han, M. (2011). Raman spectroscopic study of the effects of microbial transglutaminase on heat-induced gelation of pork myofibrillar proteins and its relationship with textural characteristics. *Food Research International, 44*(5), 1514–1520. https://doi.org/10.1016/j.foodres.2011.03.052

Egelandsdal, B., Fretheim, K., & Samejima, K. (1986). Dynamic rheological measurements on heat-induced myosin gels: Effect of ionic strength, protein concentration and addition of adenosine triphosphate or pyrophosphate. *Journal of the Science of Food and Agriculture, 37*(9), 915–926. https://doi.org/10.1002/jsfa.2740370914

Estevez, M. (2011). Protein carbonyls in meat systems: A review. *Meat Science, 89*(3), 259–27957. https://doi.org/10.1016/j.meatsci.2011.04.025

Furlán, L. T. R., Padilla, A. P., & Campderrós, M. E. (2010). Inulin like lyoprotectant of bovine plasma proteins concentrated by ultrafiltration. *Food Research International, 43*(3), 788–796. https://doi.org/10.1016/j.foodres.2009.11.015

Gao, W., Huang, Y., Zeng, X., & Brennan, M. A. (2019). Effect of soluble soybean polysaccharides on freeze-denaturation and structure of myofibrillar protein of bighead carp surimi with liquid nitrogen freezing. *International Journal of Biological Macromolecules, 135*, 839–844. https://doi.org/10.1016/j.ijbiomac.2019.05.186

Guo, L., Fang, F., Zhang, Y., Xu, D., Xu, X., & Jin, Z. (2020). Effect of glutathione on gelatinization and retrogradation of wheat flour and starch. *Journal of Cereal Science, 95*, 103061. https://doi.org/10.1016/j.jcs.2020.103061

He, Z., Liu, C., Zhao, J., Li, W., & Wang, Y. (2021). Physicochemical properties of a ginkgo seed protein-pectin composite gel. *Food Hydrocolloids, 118*, 106781. https://doi.org/10.1016/j.foodhyd.2021.106781

Herrero, A. M. (2008). Raman spectroscopy a promising technique for quality assessment of meat and fish: A review. *Food Chemistry, 107*(4), 1642–1651. https://doi.org/10.1016/j.foodchem.2007.10.014

Houston, D. K., Ding, J., Lee, J. S., Garcia, M., Kanaya, A. M., Tylavsky, F. A., … Kritchevsky, S. B. (2011). Dietary fat and cholesterol and risk of cardiovascular disease in older adults: The health ABC Study. *Nutrition, Metabolism and Cardiovascular Diseases, 21*(6), 430–437. https://doi.org/10.1016/j.numecd.2009.11.007

Hwang, J.-S., Lai, K.-M., & Hsu, K.-C. (2007). Changes in textural and rheological properties of gels from tilapia muscle proteins induced by high pressure and setting. *Food Chemistry, 104*(2), 746–753. https://doi.org/10.1016/j.foodchem.2006.11.075

Jiang, J., & Xiong, Y. L. (2016). Natural antioxidants as food and feed additives to promote health benefits and quality of meat products: A review. *Meat Science, 120*, 107–117. https://doi.org/10.1016/j.meatsci.2016.04.005

Jiao, H., & Wang, S. Y. (2000). Correlation of antioxidant capacities to oxygen radical scavenging enzyme activities in blackberry. *Journal of Agricultural and Food Chemistry, 48*(11), 5672–5676. https://doi.org/10.1021/jf000765q

Ke, Y., Wang, Y., Ding, W., Leng, Y., Lv, Q., Yang, H., … Ding, B. (2020). Effects of inulin on protein in frozen dough during frozen storage. *Food & Function, 11*(9), 7775–7783. https://doi.org/10.1039/D0FO00461H

King, L., & Lehrer, S. S. (1989). Thermal unfolding of myosin rod and light meromyosin: Circular dichroism and tryptophan fluorescence studies. *Biochemistry, 28*(8), 3498–3502. https://doi.org/10.1021/bi00434a052

Kobayashi, Y., Mayer, S. G., & Park, J. W. (2017). FT-IR and Raman spectroscopies determine structural changes of tilapia fish protein isolate and surimi under different comminution conditions. *Food Chemistry, 226*, 156–164. https://doi.org/10.1016/j.foodchem.2017.01.068

Levine, R. L., Garland, D., Oliver, C. N., Amici, A., Climent, I., Lenz, A. G., … Stadtman, E. R. (1990). Determination of carbonyl content in oxidatively modified proteins. *Methods in Enzymology, 186*, 464–478. https://doi.org/10.1016/0076-6879(90)86141

Li, F., Wu, X.-J., & Wu, W. (2020). Effects of malondialdehyde-induced protein oxidation on the structural characteristics of rice protein. *International Journal of Food Science and Technology, 55*(2), 760–768. https://doi.org/10.1111/ijfs.14379

Liu, R., Zhao, S. M., Xie, B. J., & Xiong, S. B. (2011). Contribution of protein conformation and intermolecular bonds to fish and pork gelation properties. *Food Hydrocolloids, 25*(5), 898–906. https://doi.org/10.1016/j.foodhyd.2010.08.016

Mendoza, E., García, M. L., Casas, C., & Selgas, M. D. (2001). Inulin as fat substitute in low fat, dry fermented sausages. *Meat Science, 57*(4), 387–393. https://doi.org/10.1016/S0309-1740(00)00116-9

Meyer, D., Bayarri, S., Tárrega, A., & Costell, E. (2011). Inulin as texture modifier in dairy products. *Food Hydrocolloids, 25*(8), 1881–1890. https://doi.org/10.1016/j.foodhyd.2011.04.012

Sun, W., Zhou, F., Sun, D., & Zhao, M. (2013). Effect of oxidation on the emulsifying properties of myofibrillar proteins. *Food and Bioprocess Technology, 6*(7), 1703–1712. https://doi.org/10.1007/s11947-012-0823-8

Tolano-Villaverde, I. J., Ezquerra-Brauer, J. M., Ocano-Higuera, V. M., Torres-Arreola, W., Ramirez-Wong, B., Herrera-Urbina, R., & Marquez-Rios, E. (2016).

Effect of pH and chitosan concentration on gelation of protein concentrate from giant squid mantle (*Dosidicus gigas*). *International Journal of Food Science & Technology, 51*(6), 1360–1368. https://doi.org/10.1111/ijfs.13095

Tomaschunas, M., Zörb, R., Fischer, J., Köhn, E., Hinrichs, J., & Busch-Stockfisch, M. (2013). Changes in sensory properties and consumer acceptance of reduced fat pork Lyon-style and liver sausages containing inulin and citrus fiber as fat replacers. *Meat Science, 95*(3), 629–640. https://doi.org/10.1016/j.meatsci.2013.06.002

Verheyen, C., Albrecht, A., Herrmann, J., Strobl, M., Jekle, M., & Becker, T. (2015). The contribution of glutathione to the destabilizing effect of yeast on wheat dough. *Food Chemistry, 173*, 243–249. https://doi.org/10.1016/j.foodchem.2014.10.021

Villamonte, G., Simonin, H., Duranton, F., Chéret, R., & De Lamballerie, M. (2013). Functionality of pork meat proteins: Impact of sodium chloride and phosphates under high-pressure processing. *Innovative Food Science & Emerging Technologies, 18*, 15–23. https://doi.org/10.1016/j.ifset.2012.12.001

Wang, Z., Sun, Y., Dang, Y., Cao, J., Pan, D., Guo, Y., & He, J. (2021). Water-insoluble dietary fibers from oats enhance gel properties of duck myofibrillar proteins. *Food Chemistry, 344*, 128690. https://doi.org/10.1016/j.foodchem.2020.128690

Xia, M., Chen, Y., Guo, J., Feng, X., Yin, X., Wang, L., … Ma, J. (2019). Effects of oxidative modification on textural properties and gel structure of pork myofibrillar proteins. *Food Research International, 121*, 678–683. https://doi.org/10.1016/j.foodres.2018.12.037

Xia, X., Kong, B., Liu, Q., & Liu, J. (2009). Physicochemical change and protein oxidation in porcine longissimus dorsi as influenced by different freeze-thaw cycles. *Meat Science, 83*(2), 239–245. https://doi.org/10.1016/j.meatsci.2009.05.003

Xiong, Y. L., & Guo, A. (2021). Animal and plant protein oxidation: Chemical and functional property significance. *Foods, 10*, 40–64. https://doi.org/10.3390/foods10010040

Xu, Y., Zhao, Y., Wei, Z., Zhang, H., Dong, M., Huang, M., … Zhou, G. (2020). Modification of myofibrillar protein via glycation: Physicochemical characterization, rheological behavior and solubility property. *Food Hydrocolloids, 105*, Article 105852. https://doi.org/10.1016/j.foodhyd.2020.105852

Zhang, W., Ma, J., & Sun, D. W. (2020). Raman spectroscopic techniques for detecting structure and quality of frozen foods: Principles and applications. *Critical Reviews in Food Science and Nutrition, 61*(16), 2623–2639. https://doi.org/10.1080/10408398.2020.1828814

Zhang, Y., Dong, M., Zhang, X., Hu, Y., Han, M., Xu, X., & Zhou, G. (2020). Effects of inulin on the gel properties and molecular structure of porcine myosin: A underlying mechanisms study. *Food Hydrocolloids, 108*, Article 105974. https://doi.org/10.1016/j.foodhyd.2020.105974

Zhuang, X., Han, M., Bai, Y., Liu, Y., Xing, L., Xu, X., & Zhou, G. (2018). Insight into the mechanism of myofibrillar protein gel improved by insoluble dietary fiber. *Food Hydrocolloids, 74*, 219–226. https://doi.org/10.1016/j.foodhyd.2017.08.015